Trans. Phenom. Nano Micro Scales, 7(2): 120-129, Summer and Autumn 2019
DOI: 10.22111/tpnms.2019.21469.1128

ORIGINAL RESEARCH PAPER

Two-Dimensional Flow Analysis of Nanofluid through a Porous Channel with Suction/Injection at Slowly Expanding/Contracting Walls using Variation of Parameter Method

Gbeminiyi Musibau Sobamowo**, Akin Akinshilo, Ahmed Amao Yinusa

Department of Mechanical Engineering, University of Lagos, Akoka, Lagos, Nigeria

Received 14 August 2017; revised 27 January 2019; accepted 2 February 2019; available online 29 July 2019

ABSTRACT: In this work, variation of parameter method is applied to study two-dimensional flow of nanofluid in a porous channel through slowly deforming walls with suction or injection. The results of the developed approximate analytical solution using the variation of parameter method is verified with the results of numerical solution using fourth-order Runge-Kutta method coupled with shooing techniques. Thereafter, parametric studies are carried. The graphical illustrations of simulated results of the approximate analytical solutions show that during the expansion, the axial velocity at the center of the channel decreases as the Reynolds number increases while the axial velocity increases slightly near the surface of the channel when the wall contracts at the same rate. Also, the axial velocity decreases at the center of the channel but increases near the wall as the wall expansion ratio increases. Due to the high accuracy of the variation of parameter method, the results given in the work may be used for benchmark analysis of the subsequent studies on laminar flow behaviour of nanofluid in a porous channel through slowly deforming with injection or suction.

KEYWORDS: *Expanding or Contracting walls; Nanofluid; Porous Channel; Variation of parameter method*

INTRODUCTION

The various applications of laminar flow of nanofluid through a porous channel or pipe with contracting or expanding permeable walls have continued to arouse research interests in fluid dynamics analysis. Based on the applications of transport of biological fluids through contracting or expanding vessels such as in the, kidneys and lungs internal filtration, porous diaphragms synchronous pulsation, lymphatics internal flow, respiratory system air circulation, various studies have been presented. Also, the industrial applications of the flow phenomena which include burning surface in the solid rocket motors, chromatography, transpiration cooling, diffusion of binary gas, movement of ground water, ion exchange and the use of gaseous diffusion for separation of ^{235}U from ^{238}U [1–8] have been subjects of investigations over the past decades. In such studies of the laminar flow process, the theoretical analysis of the flow phenomena involves the development of nonlinear second-order systems of partial differential equations. These nonlinear equations of the laminar flow through a porous channel have been solved numerically and by approximate analytical methods by different researchers in the past studies. In an earlier work, Majdalani [5] and Majdalani and Roh [6] studied the oscillatory channel flow with wall injection with the aids of asymptotic formulations using Wentzel- Krammers- Brillouin (WKB) and multiple-Scale techniques. Method of multiple-scale was adopted by Jankowski and Majdalani [9] to develop approximate analytical solution for the oscillatory channel flow with arbitrary suction. In another study [9], the same authors submitted analytical study for laminar flow in a porous channel with large wall suction and a weakly oscillatory pressure using means of the Liouville-Green transformation. A comparative method study of finite difference method and asymptotic technique (variation of parameters and small parameter perturbations) was utilized by Zhou and Majdalani [11] to examine the mean flow for slab rocket motors with regressing walls. The study established a good agreement between the numerical and approximate solutions for large values of Reynold number. However, the accuracy of the analytical scheme employed decreases when small Reynold number and large wall regression rate are considered simultaneously. Majdalani and Zhou [12] presented the flow analysis for moderate-to-large injection and suction driven channel flows with expanding or contracting walls. Nonetheless, Robinson [13], Zarturska et al. [14] and Si et al. [15,16] reported the multiple solutions associated with this problem. With the aid of method of regular perturbation, analysis of viscous flow between slowly expanding or contracting walls with weak permeability was explored by Majdalani et al. [17]. Dinarvand and Rashidi [18] employed homotopy perturbation method to analyze two dimensional viscous

✉ *Corresponding Author Email: *mikegbeminiyiprof@yahoo.com*
Tel.: +2347034717417; Note. This manuscript was submitted on August 14, 2017; approved on January 27, 2019; published online July 29, 2019.

Nomenclature

$\dot{a}$	time-dependent rate	$\bar{x}$	coordinate axis parallel to the channel walls
B_0	electromagnetic induction	$\bar{y}$	coordinate axis perpendicular to the channel walls
Ha	Hartmann number		**Greek Symbols**
$\bar{p}$	Pressure	α	dimensionaless wall dilation rate
Re	permeation Reynolds number	μ_{nf}	dynamic viscosity of the nanofluid
t	time	ρ_f	density of the fluid
$\bar{u}$	velocity component in x-direction	ρ_{nf}	density of the nanofluid
$\bar{v}$	velocity component in y-direction	ρ_s	density of the nanoparticles
V_w	fluid inflow velocity at the wall	σ	electrical conductivity
		Φ	fraction of nanoparticles in the nanofluid

flow in a rectangular domain bounded by two moving porous walls. Homotopy analysis and homotopy perturbation methods were adopted by in a recent study by Dinarvand et al. [19] to provide approximate analytical solutions to Berman's model of two-dimensional viscous flow in porous channels with wall suction or injection.

The authors submitted that the analytical solution developed through homotopy perturbation method (HPM) is not valid for extremely large Reynolds numbers. Such a weakness HPM has been earlier observed in the case of other perturbation techniques. Consequently, Xu et al. [20] applied homotopy analysis method (HAM) to develop highly accurate series approximations for two-dimensional viscous flow between two moving porous walls and obtained multiple solutions associated with this problem. Although, establishment has been made that HAM is a reliable and efficient semi-analytical scheme, it suffers from a number of limiting assumptions such as the requirements that the solution ought to conform to the so-called rule of solution expression and the rule of coefficient ergodicity. Also, it required the search of an auxiliary and unknown parameters that will accelerate the convergence and will satisfy the end boundary conditions, respectively. Such quests require to the use of a numerical method, which in principle and application, make homotopy analysis method more of semi-analytical than total analytical method such as in the case of homotopy perturbation and other traditional perturbation method.

Moreover, the approximate solutions through the homotopy analysis method are always expressed in form of large number of terms. In practice, such analytical solutions with large number of terms are not practically convenient for use by designers, scientist and engineers [21].

Variation parameter method (VPM) is an approximate analytical method which has been applied to solve linear and nonlinear differential equations. It is an highly accurate approximate analytical method which is completely reliable and physically realistic [22-27]. Therefore, in this present study, VPM is employed to critically analyze transient two-dimensional flow of viscous fluid through a porous channel with expanding/contracting walls subjected to injection or suction. The results of the VPM are verified numerically using fourth-order Runge-Kutta method coupled with shooing techniques. Thereafter, the developed approximate analytical solutions are used to study the effects of the flow parameters in the expanding or contracting porous channel.

PROBLEM FORMULATION

Consider a fully developed transient, laminar, incompressible and isothermal fluid flow in a two-dimensional porous channel bounded by two permeable surfaces that enable the nanofluid to enter or exit during successive expansions or contractions as shown in Figure 1a and 1b. One end of the channel is closed by a compliant solid membrane. Both walls are conditioned to have equal permeability and to uniformly expand at a time dependent rate, $\dot{a}(t)$. A coordinate system is chosen with the origin at the center of the channel as shown in the Figure.

The two-dimensional equations of the continuity and motion are

$$\frac{\partial \tilde{u}}{\partial \tilde{x}} + \frac{\partial \tilde{v}}{\partial \tilde{y}} = 0 \tag{1}$$

$$\rho_{nf}\left(\frac{\partial \tilde{u}}{\partial \tilde{t}} + \tilde{u}\frac{\partial \tilde{u}}{\partial \tilde{x}} + \tilde{v}\frac{\partial \tilde{u}}{\partial \tilde{y}}\right) = -\frac{\partial \tilde{p}}{\partial \tilde{x}} + \mu_{nf}\left(\frac{\partial^2 \tilde{u}}{\partial \tilde{x}^2} + \frac{\partial^2 \tilde{u}}{\partial \tilde{y}^2}\right) - \sigma B_o^2 \tilde{u} \tag{2}$$

$$\rho_{nf}\left(\frac{\partial \tilde{v}}{\partial \tilde{t}} + \tilde{u}\frac{\partial \tilde{v}}{\partial \tilde{x}} + \tilde{v}\frac{\partial \tilde{v}}{\partial \tilde{y}}\right) = -\frac{\partial \tilde{p}}{\partial \tilde{y}} + \mu_{nf}\left(\frac{\partial^2 \tilde{v}}{\partial \tilde{x}^2} + \frac{\partial^2 \tilde{v}}{\partial \tilde{y}^2}\right) \tag{3}$$

where

$$\rho_{nf} = \rho_f\left(1-\phi\right) + \rho_s\phi \tag{4}$$

$$\mu_{nf} = \frac{\mu_f}{\left(1-\phi\right)^{2.5}} \tag{5}$$

The appropriate boundary conditions assuming no slip condition are given as

$$\begin{aligned} &\tilde{y} = a(t), \quad \tilde{u} = 0, \quad \tilde{v} = -V_w = -\frac{a}{c} \\ &\tilde{y} = 0, \quad \frac{\partial \tilde{u}}{\partial \tilde{y}} = 0, \quad \tilde{v} = 0 \\ &\tilde{x} = 0, \quad \tilde{u} = 0 \end{aligned} \tag{6}$$

Where $c = \frac{\dot{a}}{V_w}$ represents the wall presence or injection /suction coefficient which is the measure of permeability

If one introduces the following stream functions and the mean flow vorticity

$$\tilde{u} = \frac{\partial \tilde{\psi}}{\partial \tilde{y}}, \quad \tilde{v} = \frac{\partial \tilde{\psi}}{\partial \tilde{x}} \tag{7}$$

The pressure term in equations 2 and 3 can be eliminated and consequently, the vorticity transport equation is obtained as

$$\begin{aligned} &\rho_{nf}\left(\frac{\partial \tilde{\xi}}{\partial \tilde{t}} + \tilde{u}\frac{\partial \tilde{\xi}}{\partial \tilde{x}} + \tilde{v}\frac{\partial \tilde{\xi}}{\partial \tilde{y}}\right) = \mu_{nf}\left(\frac{\partial^2 \tilde{\xi}}{\partial \tilde{x}^2} + \frac{\partial^2 \tilde{\xi}}{\partial \tilde{y}^2}\right) \\ &+\sigma B_o^2 \tilde{u}\frac{\partial \tilde{u}}{\partial \tilde{y}} \end{aligned} \tag{8}$$

Where

$$\tilde{\xi} = \frac{\partial \tilde{v}}{\partial \tilde{x}} - \frac{\partial \tilde{u}}{\partial \tilde{y}} \tag{9}$$

With the aid of the following similarity variables, the partial differential equation in equation 8 can be converted to ordinary differential equation

$$\tilde{u} = \frac{\mu_f x}{\rho_f H^2}\tilde{f}'(\eta,\tilde{t}), \quad \tilde{v} = \frac{-\mu_f}{\rho_f H}\tilde{f}(\eta,\tilde{t}) \tag{10}$$

where

$$\eta = \frac{\tilde{y}}{H}, \quad \tilde{f}'(\eta,\tilde{t}) = \frac{\partial \tilde{f}(\eta,\tilde{t})}{\partial \eta}$$

If one substitutes equation 9 and 10 into equation 8, a fourth order ordinary differential equation is arrived at as

$$\begin{aligned} &\tilde{f}_{\eta\eta\eta\eta} + \alpha(t)\left(\eta\tilde{f}_{\eta\eta\eta} + 3f_{\eta\eta}\right) + \tilde{f}\tilde{f}_{\eta\eta\eta} - \\ &\tilde{f}_{\eta}\tilde{f}_{\eta\eta} - \frac{\rho_{nf}a^2}{\mu_{nf}}\tilde{f}_{\eta\eta t} - Ha^2\tilde{f}_{\eta\eta} = 0 \end{aligned} \tag{11}$$

And the following boundary conditions becomes

$$\begin{aligned} &\eta = 0, \quad \tilde{f} = 0, \quad \tilde{f}_{\eta\eta} = 0 \\ &\eta = 1, \quad \tilde{f} = Re, \quad \tilde{f}_{\eta} = 0 \end{aligned} \tag{12}$$

Where $\alpha(\tilde{t}) = \frac{\rho_f a\dot{a}(\tilde{t})}{\mu_f}$ is the non-dimensional wall dilation rate.

It should be noted that the non-dimensional wall dilation rate is positive for expansion and negative for contraction. And $Re = \frac{\rho_f a V_w}{\mu_f}$ is the permeation Reynolds number.

The permeation Reynolds number is positive for injection and negative for suction.

Applying the following variables,

$$\begin{aligned} &\psi = \frac{\tilde{\psi}}{a\dot{a}}, \quad u = \frac{\tilde{u}}{\dot{a}}, \quad v = \frac{\tilde{v}}{\dot{a}}, \quad f = \frac{\tilde{f}}{Re} \quad \Rightarrow \\ &\psi = \frac{xf}{c}, \quad u = \frac{xf'}{c}, \quad v = \frac{-f}{c}, \quad c = \frac{\alpha}{Re} \end{aligned} \tag{13}$$

Equations11 and 12 are normalized as

$$\begin{aligned} &f_{\eta\eta\eta\eta} + (1-\phi)^{2.5}\left((1-\phi) + \frac{\rho_s}{\rho_f}\phi\right) \\ &\left\{\begin{aligned} &\alpha(t)\left(\eta f_{\eta\eta\eta} + 3f_{\eta\eta}\right) + Re\left(ff_{\eta\eta\eta} - f_{\eta}f_{\eta\eta}\right) \\ &-\frac{\rho_f a^2}{\mu_f}f_{\eta\eta t} \end{aligned}\right\} \\ &-Ha^2 f_{\eta\eta} = 0 \end{aligned} \tag{14}$$

Subject to the boundary conditions

$$\begin{aligned} &\eta = 0, \quad f = 0, \quad f_{\eta\eta} = 0 \\ &\eta = 1, \quad f = 1, \quad f_{\eta} = 0 \end{aligned} \tag{15}$$

Assuming $\alpha(\tilde{t}) = \frac{\rho_f a\dot{a}(\tilde{t})}{\mu_f}$ remains constant during the flow process, and f=f(η), then $f_{\eta\eta t} = 0$ and equation 14 reduces to

$$f_{\eta\eta\eta\eta}+(1-\phi)^{2.5}\left((1-\phi)+\frac{\rho_s}{\rho_f}\phi\right)\left\{\alpha(\tilde{t})\left(\eta f_{\eta\eta\eta}+3f_{\eta\eta}\right)+Re\left(ff_{\eta\eta\eta}-f_{\eta}f_{\eta\eta}\right)\right\}-Ha^2 f_{\eta\eta}=0 \quad (16)$$

With the boundary conditions unchanged as in equation15.

The Berman's model [1] for channels with stationary walls is recovered if α=*0* in the above equation 16.

METHOD OF SOLUTION: VARIATION PARAMETER METHOD

The nonlinear terms in equation 16 make it very difficult to develop exact analytical solution for the equation. Therefore, in the present study, variation of parameter method which is approximate analytical method is applied to solve the nonlinear equation. The procedure can be found in [22-25]. Following the standard procedure of variation of parameter method, one can write the solution of equation 16 for the case of negligible magnetic field as

$$f_{n+1}(\eta)=k_1+k_2\eta+k_3\frac{\eta^2}{2}+k_4\frac{\eta^3}{6}-\int_0^{\eta}\left(\frac{\eta^3}{3!}+\frac{\eta^2\xi}{2!}+\frac{\eta\xi^2}{2!}+\frac{\xi^3}{3!}\right)(1-\phi)^{2.5}\left((1-\phi)+\frac{\rho_s}{\rho_f}\phi\right)\begin{bmatrix}\alpha\left(\eta\left(f_{\eta\eta\eta}\right)_n+3\left(f_{\eta\eta}\right)_n\right)\\+Re\left(\left(ff_{\eta\eta\eta}\right)_n-\left(f_{\eta}f_{\eta\eta}\right)_n\right)\end{bmatrix}d\xi \quad (17)$$

Here, k_1, k_2, k_3, *and* k_4 are constants obtained by taking the highest order linear term of equation16 and integrating it four times to get the final form of the scheme. The above equation can also be written as

$$f_{n+1}(\eta)=f(0)+f'(0)\eta+f''(0)\frac{\eta^2}{2}+f'''(0)\frac{\eta^3}{6}-\int_0^{\eta}\left(\frac{\eta^3}{3!}+\frac{\eta^2\xi}{2!}+\frac{\eta\xi^2}{2!}+\frac{\xi^3}{3!}\right)(1-\phi)^{2.5}\left((1-\phi)+\frac{\rho_s}{\rho_f}\phi\right)\begin{bmatrix}\alpha\left(\eta\left(f_{\eta\eta\eta}\right)_n+3\left(f_{\eta\eta}\right)_n\right)+\\Re\left(\left(ff_{\eta\eta\eta}\right)_n-\left(f_{\eta}f_{\eta\eta}\right)_n\right)\end{bmatrix}d\xi \quad (18)$$

From the boundary conditions in equation 15.

$$f(0)=0,\quad f''(0)=0$$

Using the above statement and inserting the boundary conditions of equation 15 into equation 18, we have

$$f_{n+1}(\eta)=k_1\eta+\frac{k_2\eta^3}{6}-\int_0^{\eta}\left(\frac{\eta^3}{3!}+\frac{\eta^2\xi}{2!}+\frac{\eta\xi^2}{2!}+\frac{\xi^3}{3!}\right)(1-\phi)^{2.5}\left((1-\phi)+\frac{\rho_s}{\rho_f}\phi\right)\begin{bmatrix}\alpha\left(\eta\left(f_{\eta\eta\eta}\right)_n+3\left(f_{\eta\eta}\right)_n\right)\\+Re\left(\left(ff_{\eta\eta\eta}\right)_n-\left(f_{\eta}f_{\eta\eta}\right)_n\right)\end{bmatrix}d\xi \quad (19)$$

For the sake of conformity to variation of parameter analysis, equation 19 is written in form of

$$f_{n+1}(\eta)=k_1\eta+\frac{k_2\eta^3}{6}-\int_0^{\eta}\frac{\left(\frac{\eta^3}{3!}+\frac{\eta^2\xi}{2!}+\frac{\eta\xi^2}{2!}+\frac{\xi^3}{3!}\right)}{(1-\phi)^{2.5}\left((1-\phi)+\frac{\rho_s}{\rho_f}\phi\right)}\left[\alpha\left(\eta f'''_n+3f''_n\right)+Re\left(ff'''_n-f'_nf''_n\right)\right]d\xi \quad (20)$$

Table 1
Comparison of results of flow for small Reynolds number for suction and expansion

f(η) Re = 5.0, α=0.5		
η	**NM**	**VPM**
0.0	0.000000	0.000000
0.1	0.152874	0.152874
0.2	0.301551	0.301551
0.3	0.442606	0.442606
0.4	0.573196	0.573196
0.5	0.690876	0.690876
0.6	0.793373	0.793373
0.7	0.878373	0.878373
0.8	0.943297	0.943297
0.9	0.985090	0.985090
1.0	1.000000	1.000000

The verification of the approximate analytical solution through variation of parameter method (VPM) is carried out by comparing the results of the approximate analytical solution with the results of a numerical solution using fourth-order Runge-Kutta method coupled with shooing techniques. The comparisons of the results through the two different methods are shown in Table 1 and Table 2. The analysis revealed that the results obtained by VPM are in excellent agreements with the results obtained by the

numerical method. This shows that the results of VPM are completely reliable and physically realistic.

From the iterative scheme, the following series solutions can easily be deduced

$$f_0(\eta) = k_1\eta + \frac{k_2\eta^3}{6}$$

$$= k_1\eta + \frac{k_2\eta^3}{6}$$

$$\frac{-\phi)^{2.5}\left((1-\phi)+\frac{\rho_s}{\rho_f}\phi\right)k_2\eta^5}{30}$$

$$\frac{1-\phi)^{2.5}\left((1-\phi)+\frac{\rho_s}{\rho_f}\phi\right)k_2^2\eta^7}{2520}$$

$$f_2(\eta) = k_1\eta + \frac{k_2\eta^3}{6}$$

$$-\frac{\alpha k_2\eta^5}{30} + \frac{Re(1-\phi)^{2.5}\left((1-\phi)+\frac{\rho_s}{\rho_f}\phi\right)k_2^2\eta^7}{2520}$$

$$+\frac{\alpha^2\left[(1-\phi)^{2.5}\left((1-\phi)+\frac{\rho_s}{\rho_f}\phi\right)\right]^2 k_2\eta^7}{210}$$

$$+\frac{\alpha(1-\phi)^{2.5}\left((1-\phi)+\frac{\rho_s}{\rho_f}\phi\right)k_2k_1\eta^7}{630}$$

$$-\frac{\alpha Re\left[(1-\phi)^{2.5}\left((1-\phi)+\frac{\rho_s}{\rho_f}\phi\right)\right]^2 k_2^2\eta^9}{113480}$$

$$-\frac{\mathrm{Re}(1-\phi)^{2.5}\left((1-\phi)+\frac{\rho_s}{\rho_f}\phi\right)k_2^2k_1\eta^9}{45360}$$

$$-\frac{Re^2\left[(1-\phi)^{2.5}\left((1-\phi)+\frac{\rho_s}{\rho_f}\phi\right)\right]^2 k_2^3\eta^{11}}{2494800}$$

$$+\frac{\alpha^2 Re\left[(1-\phi)^{2.5}\left((1-\phi)+\frac{\rho_s}{\rho_f}\phi\right)\right]^3 k_2^2\eta^{11}}{178200}$$

$$-\frac{\alpha Re^2\left[(1-\phi)^{2.5}\left((1-\phi)+\frac{\rho_s}{\rho_f}\phi\right)\right]^3 k_2^3\eta^{13}}{16216200}$$

$$+\frac{Re^3\left[(1-\phi)^{2.5}\left((1-\phi)+\frac{\rho_s}{\rho_f}\phi\right)\right]^3 k_2^4\eta^{15}}{247665600} \quad (21)$$

Similarly, the other iterations $f_3(\eta)$, $f_4(\eta)$, $f_5(\eta)$, $f_6(\eta)$, $f_7(\eta)$,…$f_{15}(\eta)$ are obtained

$$f(\eta) = k_1\eta + \frac{k_2\eta^3}{6}$$

$$-\frac{\alpha k_2\eta^5}{30} + \frac{Re(1-\phi)^{2.5}\left((1-\phi)+\frac{\rho_s}{\rho_f}\phi\right)k_2^2\eta^7}{2520}$$

$$+\frac{\alpha^2\left[(1-\phi)^{2.5}\left((1-\phi)+\frac{\rho_s}{\rho_f}\phi\right)\right]^2 k_2\eta^7}{210}$$

$$+\frac{\alpha(1-\phi)^{2.5}\left((1-\phi)+\frac{\rho_s}{\rho_f}\phi\right)k_2k_1\eta^7}{630}$$

$$-\frac{\alpha Re\left[(1-\phi)^{2.5}\left((1-\phi)+\frac{\rho_s}{\rho_f}\phi\right)\right]^2 k_2^2\eta^9}{113480}$$

$$-\frac{\mathrm{Re}(1-\phi)^{2.5}\left((1-\phi)+\frac{\rho_s}{\rho_f}\phi\right)k_2^2k_1\eta^9}{45360}$$

$$-\frac{Re^2\left[(1-\phi)^{2.5}\left((1-\phi)+\frac{\rho_s}{\rho_f}\phi\right)\right]^2 k_2^3\eta^{11}}{2494800}$$

$$+\frac{\alpha^2 Re\left[(1-\phi)^{2.5}\left((1-\phi)+\frac{\rho_s}{\rho_f}\phi\right)\right]^3 k_2^2\eta^{11}}{178200}$$

$$-\frac{\alpha Re^2\left[(1-\phi)^{2.5}\left((1-\phi)+\frac{\rho_s}{\rho_f}\phi\right)\right]^3 k_2^3\eta^{13}}{16216200}$$

$$+\frac{Re^3\left[(1-\phi)^{2.5}\left((1-\phi)+\frac{\rho_s}{\rho_f}\phi\right)\right]^3 k_2^4\eta^{15}}{247665600} \quad (22)$$

Where the constants k_1 and k_2 are determined using the boundary conditions in equation15 i.e.

$$f(1) = 1, \quad f'(1) = 0$$

Table 2
Comparison of results of flow for small Reynolds number with suction and expansion

f′(η): Re = 5.0, α=0.5		
η	**NM**	**VPM**
0.0	1.536154	1.536154
0.1	1.151411	1.151411
0.2	1.453855	1.453855
0.3	1.362554	1.362554
0.4	1.245207	1.245207
0.5	1.104631	1.104631
0.6	0.941489	0.941489
0.7	0.754210	0.754210
0.8	0.539188	0.539188
0.9	0.290458	0.290458
1.0	0.000000	0.000000

Also, the developed solutions are used for parametric study in the expanding or contracting porous channel with injection and suction. The Reynold number (*Re*) is represented as "*R*" in the Figures.

Effects of permeation Reynolds number and non-dimensional wall dilation rate on the dimensionless flow velocities are shown in Figure2. Effects of Reynolds number, Re, on the velocity at constant non-dimensional wall dilation rate on the dimensionless axial velocity are displayed in Figure 2(a-d), 3(a-d), 4a and 4b. The figures show that during the expansion, the axial velocity at the center of the channel decreases as the Reynolds number increases while the axial velocity increases slightly near the surface of the channel when the wall contracts at the same rate. Also, the axial velocity decreases at the center of the channel but increases near the wall as the wall expansion ratio increases.

Also, the first-order derivatives of *f(1)* is developed as

$$
\begin{aligned}
f'(\eta) &= k_1\eta + \frac{k_2\eta^2}{2} - \frac{\alpha k_2\eta^4}{6} \\
&+ \frac{Re(1-\phi)^{2.5}\left((1-\phi)+\frac{\rho_s}{\rho_f}\phi\right)k_2^2\eta^7}{360} \\
&+ \frac{\alpha^2\left[(1-\phi)^{2.5}\left((1-\phi)+\frac{\rho_s}{\rho_f}\phi\right)\right]^2 k_2\eta^6}{30} \\
&+ \frac{\alpha(1-\phi)^{2.5}\left((1-\phi)+\frac{\rho_s}{\rho_f}\phi\right)k_2k_1\eta^6}{90} \\
&- \frac{9\alpha Re\left[(1-\phi)^{2.5}\left((1-\phi)+\frac{\rho_s}{\rho_f}\phi\right)\right]^2 k_2^2\eta^8}{113480} \\
&- \frac{\mathrm{Re}(1-\phi)^{2.5}\left((1-\phi)+\frac{\rho_s}{\rho_f}\phi\right)k_2^2k_1\eta^9}{5040} \\
&- \frac{Re^2\left[(1-\phi)^{2.5}\left((1-\phi)+\frac{\rho_s}{\rho_f}\phi\right)\right]^2 k_2^3\eta^{11}}{226800} \\
&+ \frac{\alpha^2 Re\left[(1-\phi)^{2.5}\left((1-\phi)+\frac{\rho_s}{\rho_f}\phi\right)\right]^3 k_2^2\eta^{11}}{16200} \\
&- \frac{\alpha Re^2\left[(1-\phi)^{2.5}\left((1-\phi)+\frac{\rho_s}{\rho_f}\phi\right)\right]^3 k_2^3\eta^{13}}{1247400} \\
&+ \frac{Re^3\left[(1-\phi)^{2.5}\left((1-\phi)+\frac{\rho_s}{\rho_f}\phi\right)\right]^3 k_2^4\eta^{15}}{16511040} + \cdots
\end{aligned}
\tag{23}
$$

Therefore,

$$
\begin{aligned}
1 &= k_1\eta + \frac{k_2}{6} \\
&- \frac{\alpha k_2\eta^5}{30} + \frac{Re(1-\phi)^{2.5}\left((1-\phi)+\frac{\rho_s}{\rho_f}\phi\right)k_2^2}{2520} \\
&+ \frac{\alpha^2\left[(1-\phi)^{2.5}\left((1-\phi)+\frac{\rho_s}{\rho_f}\phi\right)\right]^2 k_2}{210} \\
&+ \frac{\alpha(1-\phi)^{2.5}\left((1-\phi)+\frac{\rho_s}{\rho_f}\phi\right)k_2k_1}{630} \\
&- \frac{\alpha Re\left[(1-\phi)^{2.5}\left((1-\phi)+\frac{\rho_s}{\rho_f}\phi\right)\right]^2 k_2^2}{113480} \\
&- \frac{\mathrm{Re}(1-\phi)^{2.5}\left((1-\phi)+\frac{\rho_s}{\rho_f}\phi\right)k_2^2k_1}{45360} \\
&- \frac{Re^2\left[(1-\phi)^{2.5}\left((1-\phi)+\frac{\rho_s}{\rho_f}\phi\right)\right]^2 k_2^3}{2494800} \\
&+ \frac{\alpha^2 Re\left[(1-\phi)^{2.5}\left((1-\phi)+\frac{\rho_s}{\rho_f}\phi\right)\right]^3 k_2^2}{178200} \\
&- \frac{\alpha Re^2\left[(1-\phi)^{2.5}\left((1-\phi)+\frac{\rho_s}{\rho_f}\phi\right)\right]^3 k_2^3}{16216200} \\
&+ \frac{Re^3\left[(1-\phi)^{2.5}\left((1-\phi)+\frac{\rho_s}{\rho_f}\phi\right)\right]^3 k_2^3}{247665600}
\end{aligned}
\tag{24}
$$

Figures 3, 3(a-d) show the behavior of axial velocity for different permeation Reynolds number, over a range of non-dimensional wall dilation rate. The figures show that, for every suction or injection witnessed, the velocity is optimum at the middle of the channel and near the domain, the velocity increases as the channel expands and decreases during channel contraction. That is because the fluid flow approaching the middle becomes greater to complement for the domain instigated by the expansion of the wall and consequently resulting to the greater value of the axial velocity near the center. As the wall expansion ratio increases, the velocity at the center decreases and increases near the wall. Similarly, for the case of contracting wall as shown in Figure 3(a-d) and 4a, as the contraction ratio increases, the axial velocity near the center is lowered. However, it becomes higher near the wall because the flow toward the wall becomes greater and as a result the axial velocity near the wall becomes greater.

$$0 = k_1 + \frac{k_2}{2} - \frac{\alpha k_2}{6} + \frac{Re(1-\phi)^{2.5}\left((1-\phi)+\frac{\rho_s}{\rho_f}\phi\right)k_2^2}{360} + \frac{\alpha^2\left[(1-\phi)^{2.5}\left((1-\phi)+\frac{\rho_s}{\rho_f}\phi\right)\right]^2 k_2}{30} + \frac{\alpha(1-\phi)^{2.5}\left((1-\phi)+\frac{\rho_s}{\rho_f}\phi\right)k_2k_1}{90} - \frac{9\alpha Re\left[(1-\phi)^{2.5}\left((1-\phi)+\frac{\rho_s}{\rho_f}\phi\right)\right]^2 k_2^2}{113480} - \frac{\mathrm{Re}(1-\phi)^{2.5}\left((1-\phi)+\frac{\rho_s}{\rho_f}\phi\right)k_2^2k_1}{5040} - \frac{Re^2\left[(1-\phi)^{2.5}\left((1-\phi)+\frac{\rho_s}{\rho_f}\phi\right)\right]^2 k_2^3}{226800} + \frac{\alpha^2 Re\left[(1-\phi)^{2.5}\left((1-\phi)+\frac{\rho_s}{\rho_f}\phi\right)\right]^3 k_2^2}{16200} - \frac{\alpha Re^2\left[(1-\phi)^{2.5}\left((1-\phi)+\frac{\rho_s}{\rho_f}\phi\right)\right]^3 k_2^3}{1247400} + \frac{Re^3\left[(1-\phi)^{2.5}\left((1-\phi)+\frac{\rho_s}{\rho_f}\phi\right)\right]^3 k_2^4}{16511040} + \ldots \quad (25)$$

Equations 24 and 25 are solved simultaneously for differe-nt parameters of α and Re to determine constants k_1 and k_2.

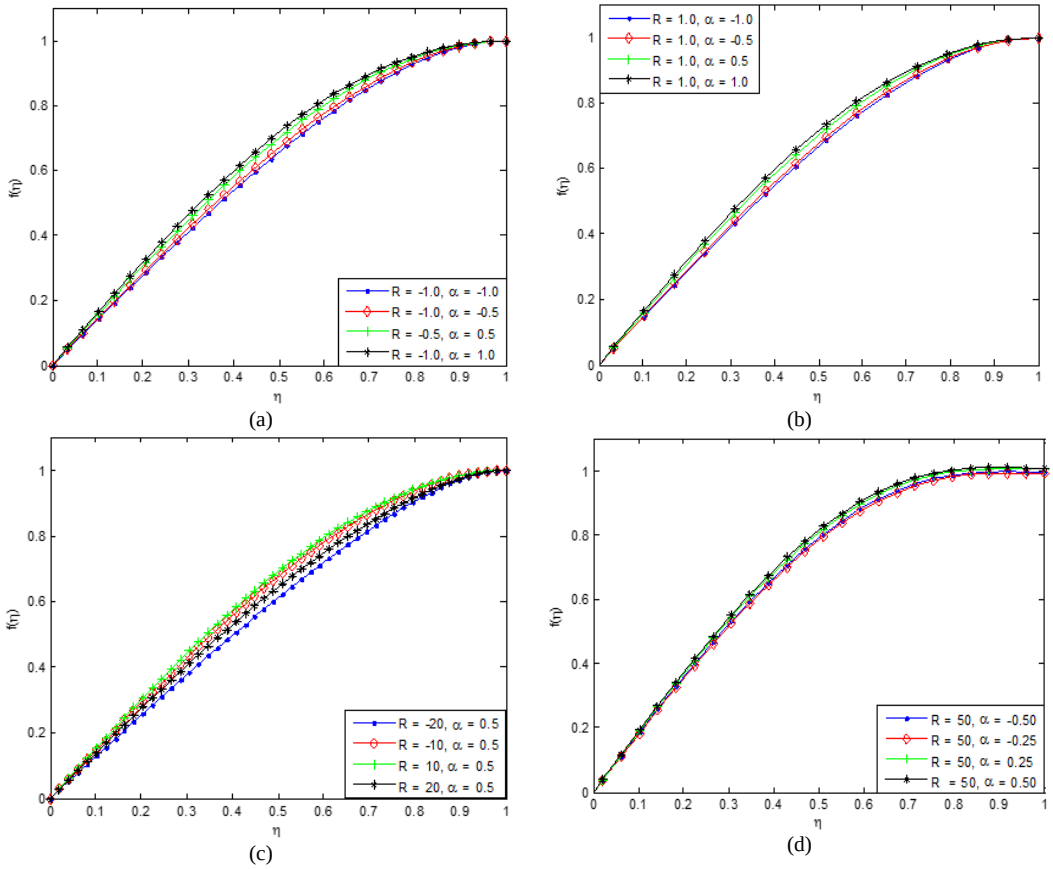

Fig. 2. Variation of f (η) for different expansion and contraction ratio, α and different small values of Reynold number

So, both the expansion and suction through the wall reinforce the flow through the channel with as similar effect for contraction and injection through the surface.

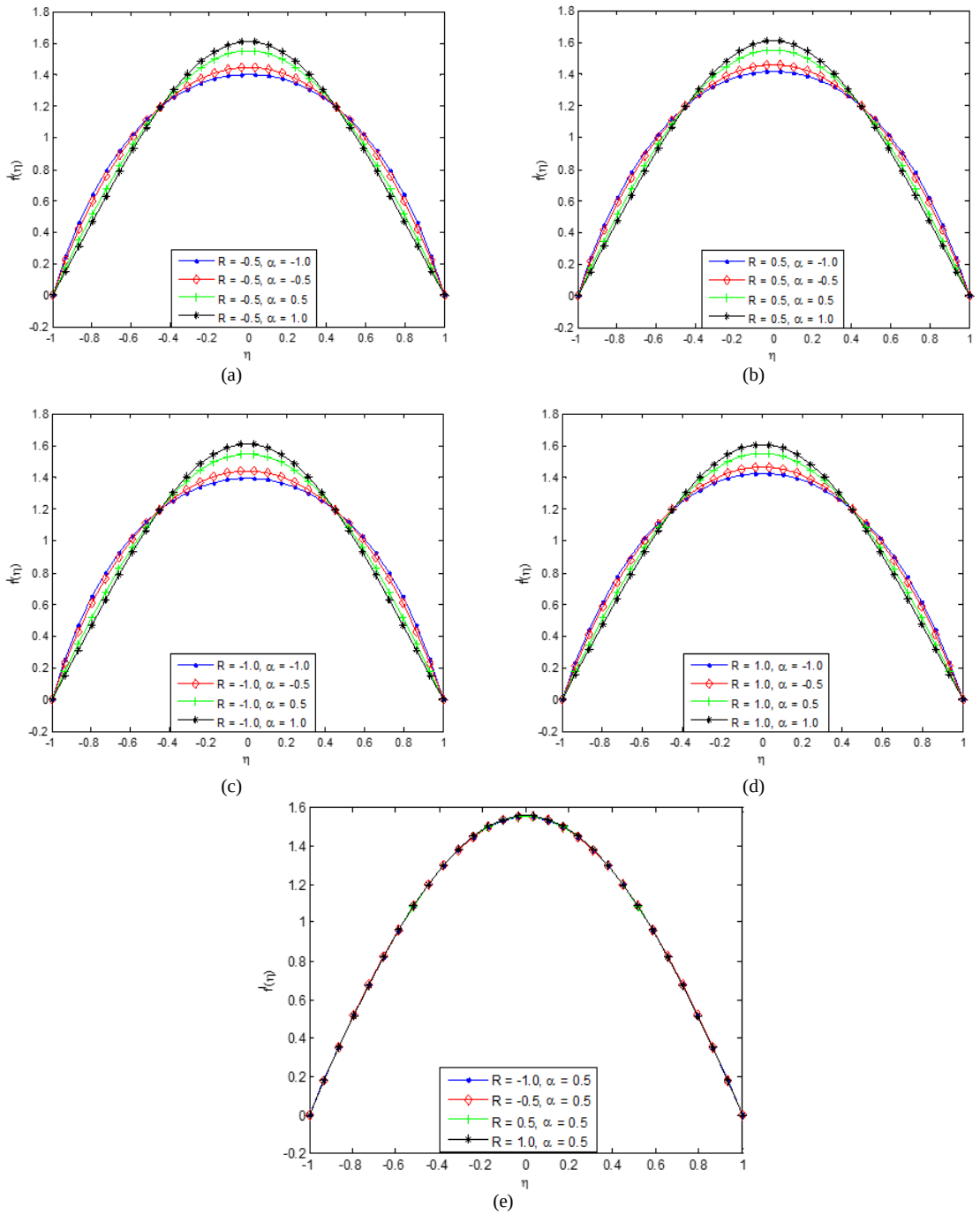

Fig. 3. Variation of f' (η) for different expansion and contraction ratio, α and different small values of Reynold number

The results of the present study show that for every level of injection or suction, in the case of expanding wall, increasing expansion ratio leads to higher axial velocity near the center and the lower axial velocity near the wall.

CONCLUSION

In this work, variation parameter method has been applied to analyze two-dimensional unsteady flow of viscous fluid in a porous channel through deforming walls with large suction or injection. Through the parametric studies, it was established that increase in the Reynolds number decreases the axial velocity at the center of the channel during the expansion while the axial velocity increases slightly near the surface of the channel when the wall contracts at the same rate. Also, as the wall expansion ratio increases, the velocity at the center decreases and increases near the wall. For every level of injection or suction, in the case of expanding wall, increasing expansion ratio leads to higher axial velocity near the center and the

lower axial velocity near the wall. It is hoped that the work will help and advance the understanding the laminar flow of nanofluid in a porous channel through slowly expanding or contracting walls with injection or suction.

REFERENCES

[1] Berman AS. Laminar flow in channels with porous walls. Journal of Applied physics. 1953 Sep;24(9):1232-5.

[2] Terrill RM. Laminar flow in a uniformly porous channel," The Aeronautical Quarterly, 1964;15: 299–310.

[3] Terrill RM. Laminar flow in a uniformly porous channel with large injection," Aeronaut. Quarterly. 1965; 16: 323–332.

[4] Dauenhauer EC and Majdalani J. Exact self-similarity solution of the Navier-Stokes equations for a porous channel with orthogonally moving walls," Physics of Fluids, 2003; 15(6):1485–1495.

[5] Majdalani, J. The oscillatory channel flow with arbitrary wall injection. Zeitschrift fur Angewandte Mathematik und Physik, 2001; 52(1) 1: 33–61.

[6] Majdalani J. and Roh, TS. The oscillatory channel flow with large wall injection. Proceedings of the Royal Society of London. Series A, 2000; 456(1999): 1625–1657.

[7] Majdalani J. and van Moorhem WK. Multiple-scales solution to the acoustic boundary layer in solid rocket motors. Journal of Propulsion and Power, 1997;13(2):186–193.

[8] Oxarango L., Schmitz P. and Quintard M. Laminar flow in channels with wall suction or injection: a new model to study multi-channel filtration systems. Chemical Engineering Science,2004;59(5): 1039–1051.

[9] Jankowski TA and Majdalani, J. Symmetric solutions for the oscillatory channel flow with arbitrary suction. Journal of Sound and Vibration, 2006; 294(4):880–893.

[10] Jankowski A. and Majdalani J. Laminar flow in a porous channel with large wall suction and a weakly oscillatory pressure. Physics of Fluids. 2002; 14(3):1101–1110.

[11] Zhou and Majdalani J. Improved mean-flow solution for slab rocket motors with regressing walls. Journal of Propulsion and Power, 2002; 18(3):703–711.

[12] Majdalani J. and Zhou C. Moderate-to-large injection and suction driven channel flows with expanding or contracting walls. Zeitschrift fur Angewandte Mathematik und Mechanik, 2003;83(3):181–196.

[13] Robinson, WA. The existence of multiple solutions for the laminar flow in a uniformly porous channel with suction at both walls, J. Eng. Math. 1976; 10: 23–40.

[14] Zaturska MB, Drazin, PG. and Banks WHH, On the flow of a viscous fluid driven along a channel by suction at porous walls. Fluid Dynamics Research, 1988; 4(3): 151–178.

[15] Si XH, Zheng LC, Zhang XX, Chao Y. Existence of multiple solutions for the laminar flow in a porous channel with suction at both slowly expanding or contracting walls. Int. J. Miner. Metal. Mater. 2011;11: 494-501.

[16] Si XH, Zheng LC, Zhang XX, Li M. Yang JH., Chao Y. Multiple solutions for the laminar flow in a porous pipe with suction at slowly expanding or contracting wall. Appl. Math. Comput.2011; 218: 3515-3521.

[17] Majdalani J., Zhou C. and Dawson CA. Two-dimensional viscous flow between slowly expanding or contracting walls with weak permeability. Journal of Biomechanics, 2002; 35(10): 1399–1403.

[18] Dinarvand S. and Rashidi, M.M. A reliable treatment of a homotopy analysis method for two dimensional viscous flow in a rectangular domain bounded by two moving porous walls," Nonlinear Analysis: Real World Applications. 2010; 11(3):1502–1512.

[19] Dinarvand S., Doosthoseini A., Doosthoseini E. and Rashidi M. M. Comparison of HAM and HPM methods for Berman's model of two-dimensional viscous flow in porous channel with wall suction or injection. Advances in Theoretical and Applied Mechanics, 2008; 1(7): 337–347.

[20] Xu J., Lin ZL, Liao SJ, Wu JZ and Majdalani J. Homotopy based solutions of the Navier-Stokes equations for a porous channel with orthogonally moving walls. Phys. Fluids 2010; 22, 053601.

[21] Sobamowo MG. Thermal analysis of longitudinal fin with temperature-dependent properties and internal heat generation using Galerkin's method of weighted residual. Applied Thermal Engineering 2016; 99:1316–1330.

[22] Noor, MA., Mohyud-Din ST. Waheed. A. Variation of parameters method for solving fifth-order boundary value problems. Appl Math Inf Sci 2008;2:135–41

[23] Noor, MA., Mohyud-Din ST. Waheed. A. Variation of parameter method for solving sixth-order boundary value problems. Commun Korean Math Soc 2009;24:605–15

[24] Mohyud-Din ST, Noor, MA.,. Waheed A. Variation of parameter method for initial and boundary value problems. World Appl Sci J 2010;11:622–39

[25] Mohyud-Din ST, Noor, MA.,. Waheed A. Modified variation of parameters method for second-order integro-differential equations and coupled systems. World Appl Sci J 2009;6:1139–46

[26] Ramos J. On the variational iteration method and other iterative techniques for nonlinear differential equations. Appl Math Comput 2008;199:39–69.

[27] Ahmed N., Jan SU, Khan U., Mohyub-Din. ST. Heat transfer analysis of third-grade fluid flow between parallel plates: Analytical solutions. Int. J. Appl. Comput. Math, 2015

[28] Fakour M., Vahabzadeh A. and Ganji DD. Study of heat transfer and flow of nanofluid in permeable channel in the presence of magnetic field. Propulsion and Power Research 2015;4(1):50–62.